Cryomilled Zinc Sulfide: A prophylactic for Staphylococcus aureus infected wounds

Article

Cryomilled Zinc Sulfide: a prophylactic for *Staphylococcus aureus* infected wounds

Abstract

Bacterial pathogens that colonize wounds form biofilms which protect the bacteria from the effect of host immune response and antibiotics. This study examined the effectiveness of newly synthesized zinc sulfide in inhibiting biofilm development by *Staphylococcus aureus* (*S. aureus*) strains. Zinc sulfide (ZnS) was anaerobically biosynthesized to produce CompA which was further processed by cryomilling to maximize the antibacterial properties to produce CompB. The effect of the two compounds on the *S. aureus* strain AH133 were compared using zone of inhibition (ZOI) assay. The compounds were formulated in a polyethylene glycol (PEG) cream. We compared the effect of the two compounds on biofilm development by AH133 and two Methicillin-resistant *S. aureus* (MRSA) clinical isolates using the *in vitro* model of wound infection. ZOI assay revealed that CompB is more effective than CompA. At 15 mg/application, the formulated cream of either compound inhibited biofilm development by AH133 which was confirmed using confocal laser scanning microscopy. At 20 mg/application, CompB inhibited biofilm development by the two MRSA clinical isolates. To further validate the effectiveness of CompB, mice were treated using the murine model of wound infection. CFU assay and *in vivo* live imaging results strongly suggested the inhibition of *S. aureus* growth.

Keywords

ZnS Particles, anti-Biofilm, *Staphylococcus aureus*, anti-MRSA, Cryomilling

Introduction

Wounds, acute and chronic, constitute a serious challenge to the health care system. Severely burned patients are immune-compromised due to the loss of skin barriers and the induced modulation of the specific and non-specific immune responses.[1] Colonization of burned tissues by different bacterial pathogens often leads to sepsis and a high mortality rate.[2] Other chronic wounds include pressure ulcers, venous ulcers, diabetic ulcers, and neuropathic ulcers.[3,4] Incomplete removal of bacterial pathogens from the acute wound prolongs the inflammatory process, delaying the wound healing process, and potentially causing the transition of an acute wound into a chronic one.[5,6] Burn wounds may be rapidly colonized by commensal bacteria, both gram positive and gram negative.[7] On colonizing a wound, these bacteria become pathogenic, accelerating their reproduction rate.

At different infection sites, including wounds, bacteria may produce a protective structure termed a biofilm.[8] Biofilms are complex structures that envelop bacteria in a self-secreted extracellular polysaccharide matrix (EPS).[9] Within the biofilm, bacteria are protected from antibiotics and the host immune responses.[10,11] The antibiotic resistance of the biofilm may reach 100 fold higher than that of the planktonic cells, which may contribute significantly to the failure of treatment of infected acute and chronic wounds.[11-13] Antibiotic resistance among bacterial pathogens is developing at an alarming rate. Therefore, it is critical that alternative antimicrobial agents are developed that can be produced in bulk with repeatable characteristics.[14]

For this purpose, we propose a novel two-step approach for the biosynthesis of ZnS. Unlike traditional synthesis methods of ZnS, the proposed method does not require organic solvents and its basis on microbial synthesis improves the biocompatibility of the particles. The antibacterial abilities of ZnS derived from

traditional methods, such as one-pot colloidal synthesis[15] and chemical precipitation[16], have been tested on *Escherichia coli*, *Pseudomonas aeruginosa*, *Actinomycete*, *Salmonella typhi, Bacillus subtilis* and *Klebsiella planticola*, deriving promising results.[15-17] The fabrication process we used is a more eco-friendly, reproducible and economical method of biosynthesis of ZnS, augmented by cryomilling as a scalable post-processing technique. Cryomilling is the mechanical attrition of powders under cryogenic conditions,[18] which was used to decrease the particle size in this study. Smaller sized particles have larger surface to volume ratio, resulting in larger surface in direct contact with the exterior environment under the same amount of antibacterial agents, thus it is expected that agents with smaller particle size will possess higher antibacterial properties.[19]. For such cryomilled ZnS powder to be used clinically, its biocompatibility must be confirmed. Macrophages, present in almost all tissues, are normally activated during bacterial infection and inflammatory response, being responsible for the digestion of unwanted or foreign materials via phagocytosis.[20] Therefore, it is speculated that cryomilled microbially synthesized ZnS will derive an improved antibacterial response when exposed to *S. aureus* or in biofilm models, whilst not eliciting a significant macrophagic reaction.

Materials and Methods

Materials

ZnS preparation. A two-step fabrication approach was used to generate the ZnS particles. First, ZnS particles were extracellularly biosynthesized using the fast-growing metal-reducing thermophilic bacterium, *Thermoanaerobacter*, X513.[18] Media used were modified from TOR-39 medium, the ingredients were described by previous work.[19] The dissolved basal medium was boiled with N_2 gas purging and

cooled with continuous N_2 gas purging. Incubation was initiated with inoculation of glucose, thiosulfate as a sulfur source, and 2 vol. % mid-log growth X513 culture. After cell growth and development of H_2S, aliquots of zinc chloride were ($ZnCl_2$, reagent grade > 98%) dosed. The precipitate of ZnS particles was recovered by centrifugation and washed more than three times with deionized water and stored as freeze-dried solid samples. The original as-biosynthesized ZnS particles were labeled as CompA.

Part of the biosynthesized ZnS particles were then cryomilled using the freezer mill 6870 (SPEX, Metuchen, NJ, USA), which was operated under a cryogenic environment of -196°C.[21] Five grams of biosynthesized ZnS particles were used for cryomilling, and the parameters used were: 5 min precool, 8 cycles, 7 min run time for each cycle, 2 min cool time in between each two cycles and 15 counts per second (CPS) for milling. The total time period for cryomilling was 56 min.[19,21] Samples acquired using this method were labeled as CompB.

Scanning Electron Microscopy (SEM) Analysis

The morphology of ZnS particles was imaged using a JEOL JCM-6000 NeoScope Benchtop Scanning Electron Microscope (SEM) (Nikon Instruments, Elgin, IL, USA). In order to clearly observe the morphology of the samples, the images were taken under 15 kV accelerating voltage, high vacuum, and magnification of 5000X, using secondary imaging mode. The images were analyzed using the JCM-6000 software version 1.1 (Nikon Instruments, Elgin, IL, USA).

X-ray Diffraction (XRD) Analysis

The ZnS particles were analyzed using a Rigaku MiniFlex 600 X-ray Diffractometer (Rigaku Inc, Woodlands, TX, USA) to determine the particles' composition and

corresponding crystal structures. The voltage and current X-ray generator applied were 40 kV and 15 mA, with Cu as the source of X-rays. The XRD profiles were analyzed using the PDXL software version 2.1.3.4.

Bacterial Strain and Media

The strain of *S. aureus* utilized in the majority of experiments considering antibacterial action was AH133.[22] AH133 carries plasmid pCM11 which contains the gene that codes for the green fluorescent protein.[22] The strain was grown in either LB Broth or on LB Agar plates at 37 °C. To maintain the plasmid, erythromycin was incorporated in the growth medium at a concentration of 1 μg/ml. We also utilized two *S. aureus* clinical isolates; MRSA 121 and MRSA 139. The isolates were obtained from patients at Texas Tech University Medical Center, Lubbock, Texas, under a protocol approved by the Institutional Review Board.

Zone of Inhibition (ZOI) Assay

The bacteria were grown overnight in LB broth and diluted in a fresh LB broth to an optical density (OD_{600}) of 0.5. A 100 μl aliquot containing approximately 10^8 CFU/ml was spread on the surface of the LB agar plate. Samples of the ZnS particles (50 mg/sample) were placed at three spots on the LB agar surface, with at least 24 mm (center to center) between them. The plates were incubated at 37 °C for 24 hours before assessment. The diameters of the zones of complete inhibition, including the diameter of the disk, were measured to the nearest millimeter with a ruler.

In vitro Biofilm Model

The biofilms were developed and assayed as previously described with some modifications.[8,23] Briefly, tested strains were grown overnight, washed once with

PBS, re-suspended in PBS to an OD_{600} of 0.5 (~10^8 CFU/mL), and serially diluted (10- fold). Three sterile cellulose discs with diameter of 6 mm were placed on the surface of freshly prepared LB agar with at least 24 mm (center to center) between them, and 10 µl containing 10^2-10^3 CFU of tested strain was inoculated onto each disc. The discs were then treated with either polyethylene glycol (PEG) (control) (PEG Ointment Base, B1300, Spectrum, Gardena, CA, USA) or ZnS particles in PEG to cover the disc. The plates were then incubated at 37°C for 24 hours. Following incubation, the discs were rinsed lightly to remove any unattached bacteria, and the biofilms were quantified using the CFU assay. The discs were transferred to a 1.5 ml microfuge tube in 1 ml of PBS and sonicated for 10 minutes. The tubes were then vortexed for one minute to disrupt and disperse the biofilm. Bacterial suspensions were serially diluted 10-fold in PBS, and 10 µl aliquots of each dilution and undiluted suspension were plated on LB agar. The plates were air dried and incubated at 37ºC for 24 hours before the results were read. The number of CFU/disc was determined as described above, using the formula CFU/disc = (CFU counted × dilution factor) × 100. All experiments were done in triplicate.

Confocal Laser Scanning Microscopy (CLSM) Analysis

The biofilms were visualized using confocal laser scanning microscopy (CLSM). The biofilms were developed as described above. After 24 hours of incubation at 37ºC, the discs were gently rinsed to remove loosely attached bacteria. Visualization of the *S. aureus* AH133 biofilms was accomplished by using a Nikon A1+/AIR+ Confocal Microscope (Nikon Inc., Melville, NY, USA) with images acquired at 2 µm intervals through the biofilms. Two and/or three-dimensional images were acquired using the Nis Elements Imaging software v. 4.20 (Nikon Inc., Melville, NY, USA). Several

image stacks of each biofilm were examined by CLSM, and the images were analyzed as previously described.[24] Experiments were done in triplicate.

Confirming the Cytocompatibility of ZnS

A murine macrophagic cell line (RAW 264.7) was used to test the cytocompatibility of CompA and CompB. The cells, at passage 10, were cultivated in standard DMEM medium (SigmaAldrich, Irvine, UK) supplemented with 10% FBS (Invitrogen, Paisley, UK) and 1% penicillin/streptomycin (100U/ml/100 µg/ml, Invitrogen, Paisley, UK). When confluent, cells were trypsinized, counted and subsequently seeded into a 96-well plate at the concentration of $3x10^4$ cells/well in a volume of 100µl of medium. Cells were then incubated for 24 hours at 37 °C, 5% CO_2, and subsequently exposed to CompA and CompB. Cytotoxicity was tested by treating macrophages with powder suspensions in standard medium, as seen elsewhere.[25] CompA and CompB were weighed and resuspended in standard medium at the concentration of 0.84% w/v (0.05 g powder in 6 ml of standard medium), creating StockA medium and StockB medium, respectively. Each stock medium was then transferred into a Pyrex bottle and autoclaved at 121°C for 15 minutes. StockA and StockB media were cooled to room temperature, then diluted to a final concentration of 3 µl/ml using standard medium (3 µl of Stock medium/1 ml of standard medium). The new solutions were named CompA medium and CompB medium and were then added to cell culture at 100 µl/well. Cells were incubated with CompA media and CompB media for 24 hours at 37 °C, 5% CO_2. At the end of the incubation time, CompA media and CompB media were replaced with fresh, standard medium and cells were incubated for a further 24 hours, before proceeding with the cell viability test.

In vivo Murine Model of Wound Infection

A group of three to four mice (including a control group) adult female Swiss Webster mice weighing 20-24 g was anesthetized using a mixture of isoflurane and oxygen and their backs were shaved. Shaved areas were completely cleansed with 95% ethanol and a superficial wound was created by centrally lifting the skin with surgical tweezers and removing 0.7 x 0.7 cm of skin with surgical scissors. Either control PEG or CompB/PEG gauze (1 cm^2) was placed on the wound. The gauzes were secured in place by applying a clear OPSITE dressing over the back of the mouse. Aliquots containing ~10^3 CFU of bacteria in 20 µl were injected in the area between the gauze and the wound. The mice were monitored twice a day for signs of infection or distress. After 5 days of observation, the mice were euthanized. Gauzes were removed, and the infected wound bed (this includes all infected connective tissues) was excised, weighed, and suspended in 1 ml of PBS. The extracted gauze and tissue were gently rinsed in PBS and homogenized in PBS. The biofilms were then analyzed by CFU assay. Prior to testing, the tissues were weighed and then homogenized in 2 ml of PBS. Animals were treated in accordance with the protocol approved by the Institutional Animal Care and Use Committee at Texas Tech University Health Sciences Center in Lubbock, TX.

Colony-Forming Unit Assays

Bandage: The biofilm assay was performed as previously described with some modifications.[26-28] Bacteria were grown overnight, washed once with PBS (pH 7.4), re-suspended in PBS (pH 7.4) to an optical density (OD_{600}) of 0.5 (10^8 CFU/mL), and serially diluted [10-fold]. Twenty microliter aliquots containing 10^3 colony-forming units were injected under either an untreated (control) PEG gauze, or test gauze

coated with CompB/PEG on the back of a mouse. These were allowed to grow for 5 days. Biofilms were quantified by determining the CFU per square centimeter of gauze. After removal from the mouse, each gauze piece was gently washed twice with sterile PBS to remove any planktonic bacteria. Excess PBS was drained from the gauze by touching it to a sterile filter paper and the gauze was then transferred to a sterile homogenized tube containing 2 ml of PBS for enumeration of bacteria. The gauzes were homogenized to loosen the cells within the biofilm and then vigorously vortexed 3 times for 1 min to detach the cells. Suspended cells were serially diluted (10-fold) in PBS, and 10-µL aliquots of each dilution were spotted onto LB Agar plates. The results were reported as attached CFU per a square centimeter of gauze. All experiments were done at least in triplicate.

Tissue: At the end of the experiment (5 days), the mouse was euthanatized and the tissue of the wound was removed. The tissues were weighed. This was then homogenized and used for a CFU assay in a manner similar to that used for the gauze above. The results were reported as attached CFU per gram of tissue. All experiments were done at least in triplicate.

Live Animal Imaging Studies using IVIS

After 5 days, the biofilms on the wounds of the mice were visualized and imaged using IVIS - Live Whole Animal Body Imaging System (Perkin Elmer, Massachusetts, USA) as previously described.[28] This instrument allows us to have a direct detection of pathogens infection in living animals to be monitored by bioluminescence. In this case we used bacterium, *S. aureus* Lux, that had the Lux gene incorporated into its plasmid (*S. aureus* Lux). Bioluminescence offers a method

for monitoring pathogen infections *in vivo* that is sensitive and noninvasive and requires fewer animals than conventional methodologies.

Cell Viability Assay

Cell viability was investigated using CellTiter-Blue Cell Viability Assay (Promega, Southampton, UK) after 24 and 48 hours from the end of the treatment with CompA and CompB media. Briefly, 20µl/well of the reagent were added to cells grown in a 96-wells plate, according to the manufacturer's protocol. Then, cells were incubated at 37 °C, 5% in CO_2 for 2 hours. At the end of the incubation time, the supernatant of each well was transferred in a fresh 96-wells black plate, glass bottom, and fluorescence was measured with a microplate reader (Modulus™ II Microplate Multimode Reader, Turner Biosystems, Sunnyvale, California, USA) at 560/690 nm. Cells grown in standard medium were used as controls and samples were investigated in triplicate. Results are expressed as cell viability percentage ± SD, normalized to the control. At the end of the incubation time with CompA and CompB medias, cell morphology was evaluated using bright-field microscopy (Leica Microsystem, Milton Keynes, UK), at 200x magnification.

Statistical Analysis

Results of the CFU and cell viability assays were analyzed with Prism® version 4.03 (GraphPad Software, San Diego, CA, USA) with 95% confidence intervals (CI) of the difference. Linear mixed effect model was used to model the experiment data in order to account for repeated measurements.[29,30] Shapiro-Wilk W test was used to determine the normality of the data. Levene's test was used to test equal variance between treatment groups as it can be used to compare variances between two or more groups. One-way Analysis of Variance (ANOVA) was performed to check the difference in

means between two or more treatment groups. Lastly, one-tailed and Two-tailed Student's *t*-tests were used to determine if the means between two groups are different. The statistical analyses were performed using JMP® software (SAS, Cary, NC, USA).

Results

SEM Analysis

Figures 1 (a-b) shows the morphologies of biosynthesized (CompA) and cryomilled ZnS particles (CompB). Due to particles aggregation during freeze-drying the original ZnS aggregates have irregular shape with an average diameter of 2.8 mm with standard deviation of 1.5 mm, while the cryomilled ZnS particles have an average diameter of 0.8 μm with standard deviation of 0.4 μm, which is a decrease in size in excess of three orders of magnitude. Meanwhile, the shape of the particles has been altered to more arbitrary shapes with sharp edges. Due to the decrease in size of the particles, the surface area to volume ratio has been increased.

[insert Figure 1.]

XRD Analysis

Figure 2 shows the XRD profile of the biosynthesized particles. The three major diffraction peaks correspond to the (111), (220), (311) planes of crystalline ZnS, which match the XRD profile of ZnS sphalerite. The result has shown that ZnS sphalerite has a cubic crystal structure with 5.394493 Å in unit cell dimension.

[insert Figure 2.]

Zinc Sulfide Inhibits the Planktonic Growth of S. aureus AH133. ZOI Assay

Figure 3 shows the ZOI assay result for CompA. Using the ZOI assay, ZnS CompA at a level of 50 mg created the zone of inhibition of average of 11.5 $\pm$ 0.66 mm whereas CompB produced a larger ZOI (18.87 $\pm$ 0.90 mm). These results suggest that while both compounds inhibit the growth of AH133, CompB is statistically more effective ($P < 0.005$).

[insert Figure 3.]

CompA and CompB Inhibit Biofilm Development by S. aureus AH133

Biofilms were developed and quantified as described in the Materials and Methods section. As shown in Figure 4, PEG treatment had no effect on biofilm development (control). However, at 15, 25, or 50 mg/disc, CompA and CompB completely inhibited the development of AH133 biofilm. At 10 mg/disc of CompA, the biofilm was reduced by about 4 logs (Figure 4A). However, treatment of the discs with 10 mg/disc of CompB reduced the biofilm by about 7 logs (Figure 4B). These results suggest that at a minimum concentration of 15 mg/disc, both compounds are very effective in inhibiting the development of AH133 biofilm.

[insert Figure 4.]

These results were confirmed by the visualization of the biofilm using CLSM. As shown in Figure 5 (a-d), on untreated discs and discs treated with PEG, we detected well developed mature biofilms (shown in green). In contrast, no biofilms were detected on discs treated with 15, 25, or 50 mg/disc of either Comp A or Comp B. On discs treated with CompA at a concentration of 10 mg/disc, we detected AH133 biofilm (Figure 5c). No biofilm was detected on discs treated with 10 mg/disc of

Comp B (Figure 5d) confirming that CompB is more effective in inhibiting AH133 biofilm than CompA.

[insert Figure 5.]

CompB interferes with Biofilm Development by Two Methicillin-Resistant S. aureus (MRSA) Clinical Isolates

MRSA strains (both community acquired and hospital acquired) represent major bacterial pathogens in wound infection. Routine antibiotic treatment is basically ineffective in eliminating MRSA infections. Since our results showed that CompB is more effective than Comp A, we tested the efficacy of CompB in inhibiting biofilm development by two MRSA isolates (MRSA 121 and MRSA 139) obtained at the Texas Tech University Medical Center, Lubbock Texas. As shown in Figure 6A, at 15mg/disc Comp B reduced MRSA121 biofilm significantly (about 6-fold reduction). However, it completely inhibited the biofilm formation at 20 mg/disc (Figure 6A). We obtained similar results when we examined CompB with MRSA139 (Figure 6B). With MRSA139, 10 mg of CompB reduced the biofilms by about 5-fold while 15 mg reduced it by about 8-fold (Figure 6B). These results suggest that CompB is effective in inhibiting biofilm development by the two MRSA strains.

[insert Figure 6.]

CompA is More Cytotoxic than CompB

CompA and CompB cell biocompatibility was tested by treating murine macrophages RAW264.7 cells with CompA and CompB media for 24 hours. At the end of the incubation period, cells were imaged by brightfield microscopy (Figure 7). Brightfield images revealed the presence of non-cryomilled particles in medium of cells treated

with CompA medium (Figure 7a), while the medium of cells treated with CompB (Figure 7b) appeared similar to the control. Moreover, cells incubated with CompA failed to reach full confluence (Figure 7c). CellTiter-Blue Cell Viability Assay (Figure 8) showed that after 24 hours from the end of cells incubation with CompA medium, average cell viability is reduce by 43% in comparison to the controls, considered as 100% (CompA medium cell viability = 57 ± 12%), while average of viability of cells incubated with CompB medium did not differ from controls (CompB medium cell viability = 92 ± 11%). These results were confirmed also 48 hours after the end of cells incubation with CompA and CompB media. Average of cell viability of cells incubated with CompA is reduced by 42% than controls (58 ± 12%), while average of viability of cells incubated with CompB medium did not differ from controls (CompB medium cell viability = 99.77 ± 8.04%). Viability of cells treated with CompB and CompA are statistically different ($p<0.05$). Overall, results show that there is no difference in cell morphology and cell viability between cells treated with CompB and controls, while the viability of cells incubated with CompA is reduced by more than 42%, suggesting cell cytotoxicity for CompA and an optimal biocompatibility for CompB.

[insert Figure 7.]

[insert Figure 8.]

CompB Inhibits the Growth of S. aureus in Infected Wounds

We determined the effectiveness of the cream-formulated zinc –nanoparticles (CompB) in inhibiting the growth of *S. aureus* within infected wounds. We formulated CompB in polyethylene glycol (PEG) which is water soluble, inert, non-volatile, and does not hydrolyze or deteriorate. We previously utilized this PEG in

formulating another antimicrobial agent.[26] In this study, we evaluated the effectiveness of CompB in PEG using the murine model of wound infection as previously described.[26-28] We employed live image analysis to monitor the growth of *S. aureus* within the infected wound. For this purpose, we utilized a specific *S. aureus* strain, Xen-29, which contains a single copy of the *Photorhabdus liminescens luxABCDE* operon in its chromosome.[26,28] As the strain grows within the wound, it would emit luminescence, which can be detected by the IVIS Lumina XR system with Living Image software. Once made, the wound was covered with a sterile gauge containing 400 mg of either PEG or CompB-PEG. The materials were evenly distributed on the surface of the gauze. To secure the gauze, we covered it with OpSite dressing. We then injected about 1 x 10^3 CFU of Xen-29 between the gauze and the wound. At 1 and 5 days post-infection/treatment, we briefly anesthetized the mice and visualized the wounds. As shown in Figure 9 (a-b), in mice treated with PEG only, Xen-29 colonized the wound and grew within the infected tissues. However, CompB/PEG treatment inhibited the growth of Xen-29 (Figure 9b).

[insert Figure 9.]

To confirm these results, we determined the number of microorganisms (CFU) within the gauze as well as the infected/treated tissue. Mice were infected and treated with either PEG or CompB/PEG as described above. At 24 hours post infection/treatment, mice were euthanized and the gauzes were separated and suspended in PBS. Similarly, infected/treated tissues were excised and suspended in PBS. The gauzes and tissues were homogenized and serially diluted (1:10 dilution) to determine CFU/gm of tissue or gauze. As shown in Figure 9a, *S. aureus* grew in both the gauze and the infected wound. In contrast, we did not recover any bacterium from

either the tissues or gauzes in mice that were treated with CompB/PEG (Fig.10 (A-B)). These results strongly suggest that the PEG formulated CompB inhibits the growth of *S. aureus* within the infected wound.

[insert Figure 10.]

Discussion

The results have shown the effectiveness of the suggested two-step fabrication approach for generating ZnS particles possessing antibacterial properties. It is theorized that the enhanced antibacterial properties of the cryomilled ZnS particles may originate from a direct deposition mechanism. That is, the effect that direct deposition of the particles may have on cell death.[31-33] According to Raghupathi *et al*.[31], the deposition of particles directly unto the surface of bacteria or their collection in the cytoplasm or periplasmic region leads to disruption of cellular activities. It may also cause disorder of the membrane thereby contributing towards cell death.[31] CompB, which is the cryomilled sample, showed better antibacterial effectiveness than CompA. Therefore, it is understood that the increased antibacterial effectiveness of ZnS resulted from the decrease in particle size and increase in surface-to-volume ratio that was obtained via cryomilling. As shown in Figure 3, CompB produced larger zones of bacterial inhibition than CompA. In addition, CompB was more effective than CompA in inhibiting biofilm development by the *S. aureus* strain AH133 (Figures 4 & 5 (a-d)). Furthermore, at 20 mg/disc, CompB inhibited biofilm development by the two MRSA strains (Figure 6). Consequently, the outcomes of this study direct towards defining the antibacterial mechanism of ZnS as related to the direct deposition of particles and the interaction generated between surfaces.[31]

Besides reducing the particle size, cryomilling may enhance the antimicrobial properties of CompB by introducing differences in the lattice constant. Sphalerite has a cubic crystal structure with lattice constant *c* of 0.5 nm,[34] but mechanical milling changes the crystal structure. Past research has shown that milling results in slightly higher *c* values,[35] and a lattice relaxation occurs along the axis for zinc oxide.[36] The increased *c* value has a significant effect on the amount of H_2O_2 generated from the surface of the particles, which in turn helps the inhibition of bacterial growth.[19,37] The enhanced effect of the CompB cream against *S. aureus* biofilms (in comparison with CompA) is likely due to the fact that reducing the size of the particles by cryomilling enhanced the mixing of the ZnS particles with the PEG base. Furthermore, preliminary investigations on CompB powder showed good biocompatibility when administered to RAW264.7 macrophages (Figure 8), suggesting that ZnS cryomilled powder is not likely to hyper-stimulate macrophages into a foreign-body response.

Currently used strategies to treat infected wounds include; debridement to eliminate bacterial biofilms and remove necrotic tissues, covering the wound with wound dressings to protect newly granulating tissues and help maintain moisture within the wounds, and the utilization of local and/or systemic antibiotics. While debridement removes bacterial biofilms from the wound surface, it does not eliminate bacteria deep within the underlying connective tissues. Similarly, tissue necrosis within the area surrounding the wound bed restricts the blood supply to the wound and reduces the effectiveness of systemically administered antibiotics. Topical applications, however, bring the antimicrobial agent in direct and prolonged contact with the wound pathogens and their biofilms. In addition, the antimicrobial agent may reach deeper tissues within the wound and eliminate the bacterial within these tissues. Several topical antimicrobial agents have been utilized to treat infected

wounds with variable successes.[38-40] Using the *in vitro* wound biofilm model, we previously investigated the effectiveness of three commonly used antibiotic ointments in preventing the development of *S. aureus* biofilms. These ointments included: gentamicin sulfate, mupirocin, and triple-antibiotic (bacitracin, neomycin, and polymixin B). All three ointments reduced biofilms by 0.3-2.0 log10 CFU/disc.[8] In contrast, formulated CompB completely inhibited the development of *S. aureus* biofilms including those produced by two MRSA clinical isolates (Figs. 4 & 6). In addition, formulated CompB inhibited the growth of *S. aureus* within infected wounds (Figs. 9b & 10) suggesting that CompB is a potential antimicrobial agent to treat wound infections. We plan to examine the effectiveness of the formulated CompB against other wound pathogens including*; Klebsiella pneumoniae, Staphylococcus epidermidis*, and *Acinetobacter baumannii* in our future studies.

Conclusion

A novel two-step fabrication approach yielding ZnS particles with antibacterial properties for burn wound treatment has been introduced. The ZnS particles were biologically, reproducibly and economically synthesized using the anaerobic thermophilic metal-reducing bacteria *Thermoanaerobacter* X513. Smaller sized ZnS particles were produced by milling the as-biosynthesized ZnS under a cryogenic environment for 56 min. The biosynthesized ZnS and cryomilled ZnS were proven to have a significant effect on the growth and biofilm development by *Staphylococcus aureus*. Future experiments will be conducted to examine the effectiveness of the cryomilled ZnS particles on the growth and biofilm development by other Gram-positive and Gram-negative wound pathogens.

Acknowledgements

A portion of this research was conducted at the Center for Nanophase Materials Sciences, which is a DOE Office of Science User Facility. Ji- M., D. E. G. were supported by the US Department of Energy (DOE), Advanced Manufacturing Office, Low Temperature Material Synthesis Program (CPS 24762, CPS 24764).

References

1. Alexander JW. Mechanism of immunologic suppression in burn injury. *J Trauma* 1990; 30(12 Suppl): S70-S75.

2. Markley KV. Systemic and local infection and immunity. The role of bacteria in burn mortality. *Ann N Y Acad Sci* 1968; 150: 922-930.

3. Percival SL, Emanuel C, Cutting KF, et al. Microbiology of the skin and the role of biofilms in infection. *Int Wound J* 2012; 9: 14-32.

4. Ricco JB, Thanh PL, Schneider F, et al. The diabetic foot: a review. *J Cardiovasc Surg* 2013; 54: 755-762.

5. Guo S, Dipietro LA. Factors affecting wound healing. *J Dent Res* 2010; 89: 219-229.

6. Edwards R and Harding KG. Bacteria and wound healing. *Curr Opin Infect Dis* 2004; 17: 91-96.

7. Church D, Elsayed S, Reid O, et al. Burn wound infections. *Clin Microbiol Rev* 2006; 19: 403-434.

8. Hammond AA, Miller KG, Kruczek CJ, et al. An in vitro biofilm model to examine the effect of antibiotic ointments on biofilms produced by burn wound bacterial isolates. *Burns* 2011; 37: 312-321.

9. Donlan RM and Costerton JW. Biofilms: survival mechanisms of clinically relevant microorganisms. *Clin Microbiol Rev* 2002; 15: 167-193.
10. Stewart PS. Mechanisms of antibiotic resistance in bacterial biofilms. *Int J Med Microbiol* 2002; 292: 107-113.

11. Kennedy P, Brammah S, and Wills E. Burns, biofilm and a new appraisal of burn wound sepsis. *Burns* 2010; 36: 49-56.

12. Percival SL, Hill KE, Malic S, et al. Antimicrobial tolerance and the significance of persister cells in recalcitrant chronic wound biofilms. *Wound Repair Regen* 2011; 19: 1-9.

13. Stoodley P, Sauer K, Davies DG, et al. Biofilms as complex differentiated communities.

Annu Rev Microbiol 2002; 56: 187-209.

14. Jones KE, Patel NG, Levy MA, et al. Global trends in emerging infectious diseases. *Nature* 2008; 451: 990-993.

15. Li G, Zhai J, Li D, et al. One-pot synthesis of monodispersed ZnS nanospheres with high antibacterial activity. *Journal of Materials Chemistry* 2010; 20: 9215-9219.

16. Amir GR, Fatahian S, and Kianpour N. Investigation of ZnS Nanoparticle Antibacterial Effect. *Current Nanoscience* 2014;10: 796-800.

17. Moon JW, Ivanov IN, Duty CE, et al. Scalable economic extracellular synthesis of CdS nanostructured particles by a non-pathogenic thermophile. *J Ind Microbiol Biotechnol* 2013; 40: 1263-1271.

18. Moon JW, Ivanov IN, Joshi PC, et al. Scalable production of microbially mediated zinc sulfide nanoparticles and application to functional thin films. *Acta Biomater* 2014; 10: 4474-4483.

19. Salah N, Habib SS, Khan ZH, et al. High-energy ball milling technique for ZnO nanoparticles as antibacterial material. *Int J Nanomedicine* 2011; 6: 863-869.

20. Aderem A and Underhill DM. Mechanisms of phagocytosis in macrophages. *Annu Rev Immunol* 1999; 17: 593-623.

21. Witkin DB and Lavernia EJ. Synthesis and mechanical behavior of nanostructured materials via cryomilling. *Progress in Materials Science* 2006; 51: 1-60.

22. Malone CL, Boles BR, Lauderdale KJ, et al. Fluorescent reporters for Staphylococcus aureus. *J Microbiol Methods* 2009; 77: 251-260.

23. Tran PL, Hammond AA, Mosley T, et al. Organoselenium coating on cellulose inhibits the formation of biofilms by Pseudomonas aeruginosa and Staphylococcus aureus. *Appl Environ Microbiol* 2009; 75: 3586-3592.

24. Tran PL, Lowry N, Campbell T, et al. An organoselenium compound inhibits Staphylococcus aureus biofilms on hemodialysis catheters in vivo. *Antimicrob Agents Chemother* 2012; 56: 972-978.

25. Varmette EA, Nowalk JR, Flick LM, et al. Abrogation of the inflammatory response in LPS-stimulated RAW 264.7 murine macrophages by Zn- and Cu-doped bioactive sol-gel glasses. *J Biomed Mater Res A* 2009; 90: 317-325.

26. Miller KG, Tran PL, Haley CL, et al. Next science wound gel technology, a novel agent that inhibits biofilm development by gram-positive and gram-negative wound pathogens. *Antimicrob Agents Chemother* 2014; 58: 3060-3072.

27. Rumbaugh KP, Diggle SP, Watters CM, et al. Quorum sensing and the social evolution of bacterial virulence. *Curr Biol* 2009; 19: 341-345.

28. Tran PL, Huynh E, Hamood AN, et al. The ability of a colloidal silver gel wound dressing to kill bacteria in vitro and in vivo. *J Wound Care* 2017; 26(sup4): S16-S24.

29. Malhotra-Kumar S, Lammens C, Coenen S, et al. Effect of azithromycin and clarithromycin therapy on pharyngeal carriage of macrolide-resistant streptococci in healthy volunteers: a randomised, double-blind, placebo-controlled study. *Lancet* 2007; 369: 482-490.

30. Bergman M, Huikko S, Pihlajamaki M, et al. Effect of macrolide consumption on erythromycin resistance in Streptococcus pyogenes in Finland in 1997-2001. *Clin Infect Dis* 2004; 38: 1251-1256.

31. Raghupathi KR, Koodali RT, and Manna AC. Size-dependent bacterial growth inhibition and mechanism of antibacterial activity of zinc oxide nanoparticles. *Langmuir* 2011; 27: 4020-4028.

32. Franklin NM, Rogers NJ, Apte SC, et al. Comparative toxicity of nanoparticulate ZnO, bulk ZnO, and ZnCl2 to a freshwater microalga (Pseudokirchneriella subcapitata): the importance of particle solubility. *Environ Sci Technol* 2007; 41: 8484-8490.

33. Lipovsky A, Levitski L, Tzitrinovich Z, et al. The different behavior of rutile and anatase nanoparticles in forming oxy radicals upon illumination with visible light: an EPR study. *Photochem Photobiol* 2012; 88: 14-20.

34. Engel GE and Needs RJ. Calculations of the structural properties of cubic zinc sulfide. *Phys Rev B Condens Matter* 1990; 41: 7876-7878.

35. Bao D, Gu H, and Kuang A. Sol-gel-derived c-axis oriented ZnO thin films. *Thin Solid Films* 1998; 312: 37-39.

36. Maki H, Ichinose N, Ohashi N, et al. The lattice relaxation of ZnO single crystal (0001) surface. *Surface Science* 2000; 457: 377-382.

37. Yamamoto O, Komatsu M, Sawai J, et al. Effect of lattice constant of zinc oxide on antibacterial characteristics. *J Mater Sci Mater Med* 2004; 15: 847-851.

38. Kostenko V, Lyczak J, Turner K, et al. Impact of silver-containing wound dressings on bacterial biofilm viability and susceptibility to antibiotics during prolonged treatment. *Antimicrob Agents Chemother* 2010; 54: 5120-5131.

39. Bjarnsholt T, Kirketerp-Moller K, Kristiansen S, et al. Silver against Pseudomonas aeruginosa biofilms. *APMIS* 2007; 115: 921-928.

40. Dowd SE, Sun Y, Smith E, et al. Effects of biofilm treatments on the multi-species Lubbock chronic wound biofilm model. *J Wound Care* 2009; 18: 508, 10-12.

Figure Captions

Figure 1. SEM images of (a) original freeze-dried ZnS particles (CompA), with diameters of around 2.8 mm and standard deviation of 1.5 mm and (b) cryomilled ZnS particles (CompB) with average diameter of 0.8 μm and standard deviation of 0.4 μm.

Figure 2. XRD profile of the synthesized ZnS particles with three major peaks corresponding to the (111), (220) and (311) crystal planes that match the crystal structure of ZnS sphalerite.

Figure 3. CompA (A) and CompB (B) inhibit the planktonic growth of *S. aureus* strain AH133. The analysis was done using the ZOI assay.

Figure 4. ZnS ointment inhibits biofilm development by the *S. aureus* strain AH133. Cellulose disks were inoculated with AH133 and covered with pieces of sterile gauze containing either CompA-formulated ointment (A) or CompB-formulated ointment (B). Some disks were covered with pieces of sterile gauze containing PEG (ointment control) while others were covered with sterile gauze (untreated controls). Values represent the means (plus/minus) SE of three independent experiments.

Figure 5. CLSM visualization of the biofilm formed on disks inoculated with AH133 and treated with either CompA-formulated ointment (A) or CompB-formulated ointment (B). a, untreated control; b, discs treated with PEG (cream base); c, discs treated with 10 mg of CompA (A); d, discs treated with 10 mg of CompB (B). Experiments were conducted as described in Figure 4.

Figure 6. CompB-formulated cream inhibits biofilm development by the *S. aureus* methicillin resistant (MRSA) clinical isolates 121 (A) and 139 (B). Experiments were conducted as described in Figure 4. Disks were treated with 10, 15, or 20 mg of CompB-formulated in PEG. Values represent the means of three independent experiments (plus/minus) SE.

Figure 7. Bright field pictures of RAW 264.7 cells the day after incubation with (a) CompA medium (uncryomilled ZnS)**,** (b) CompB medium (cryomilled ZnS), and (c) Control cells (standard medium). Scale bar=20μm, 200x magnification.

Figure 8. Metabolic activity was measured 24h and 48h after indicated exposure conditions. Diagrams display mean ± SD of three independent experiments.

Figure 9. Mice were treated as described in The Murine Model of Wound Infection. In vivo live imaging of (a) a representative mouse examined 1 and 5 days after treatment with PEG as a control and (b) a representative mouse examined 1 and 5 days after treatment with CompB/PEG. Images shown are representative of 1 of the 3 separate replicate experiments.

Figure 10. CompB/PEG inhibits *S. aureus* biofilm formation within the infected wound. Mice were treated as described in Figure 9. At 24 h post infection/treatment, mice were euthanized and the gauze and 15-mm depth samples of wound bed tissue were recovered, and homogenized. The homogenates were serially diluted 10-fold and 10-μl aliquots of each dilution were spotted onto LB agar plates. The numbers of

CFU/cm^2 of gauze or CFU/g of tissue (A) or CFU/cm^2 of gauze (B) as described within the text. Values in the graphs represent the means 3 independent experiments ± SEM; ****, P = 0.0001.

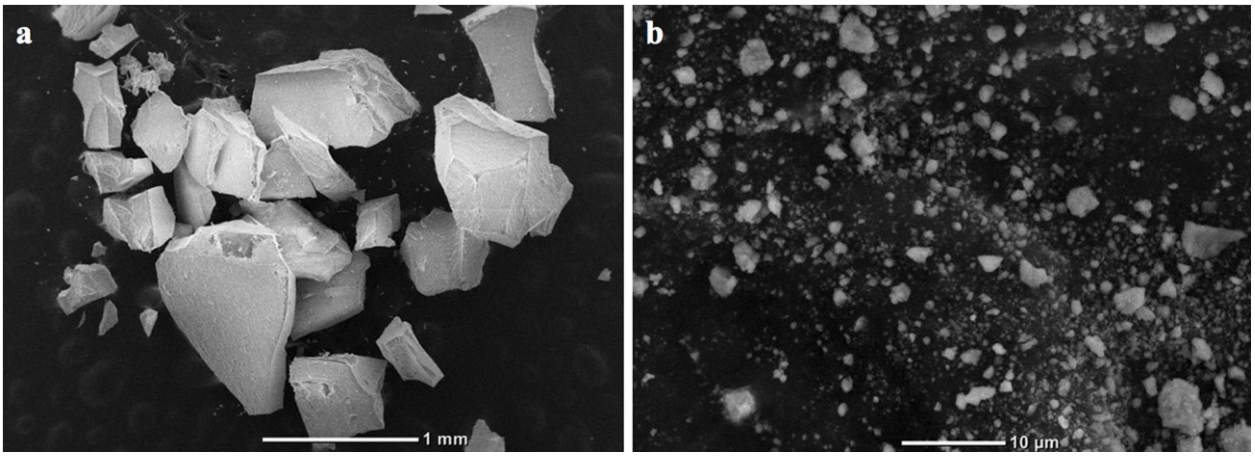

Figure 2. SEM images of (a) original freeze-dried ZnS particles (CompA), with diameters of around 2.8 mm and standard deviation of 1.5 mm and (b) cryomilled ZnS particles (CompB) with average diameter of 0.8 µm and standard deviation of 0.4 µm.

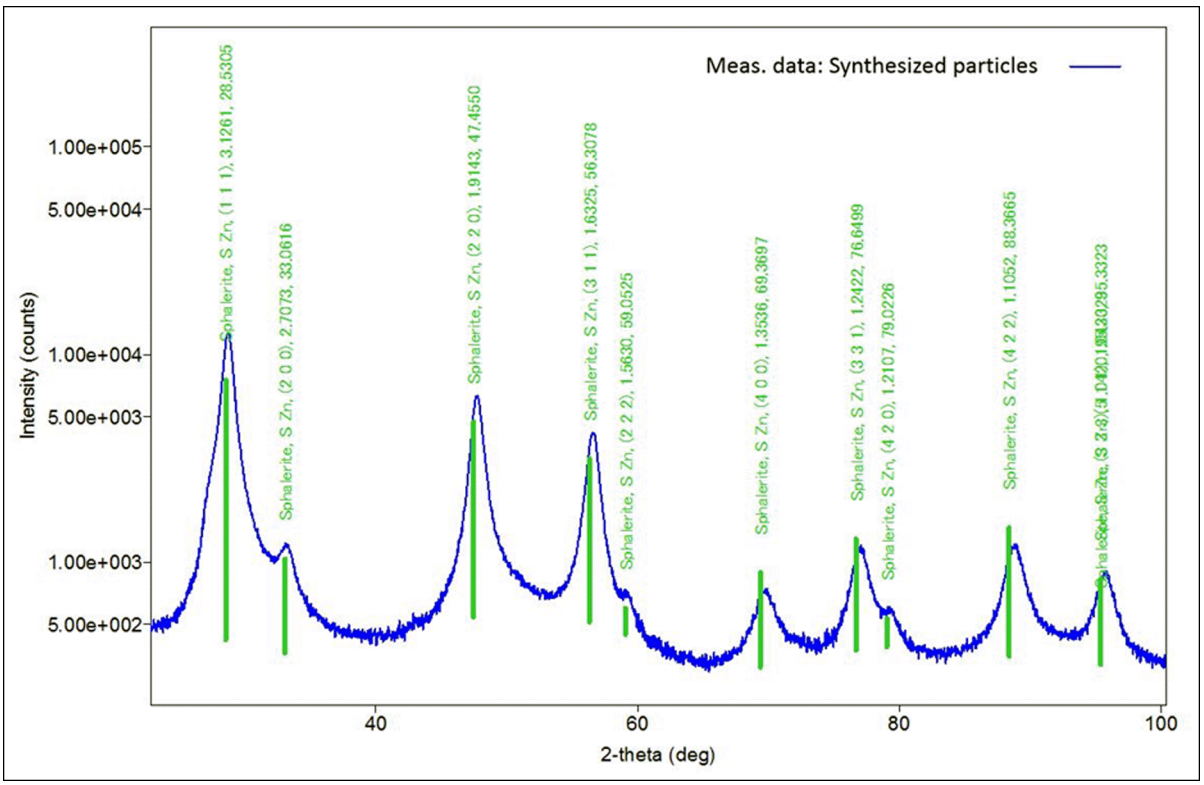

Figure 2. XRD profile of the synthesized ZnS particles with three major peaks corresponding to the (111), (220) and (311) crystal planes that match the crystal structure of ZnS sphalerite.

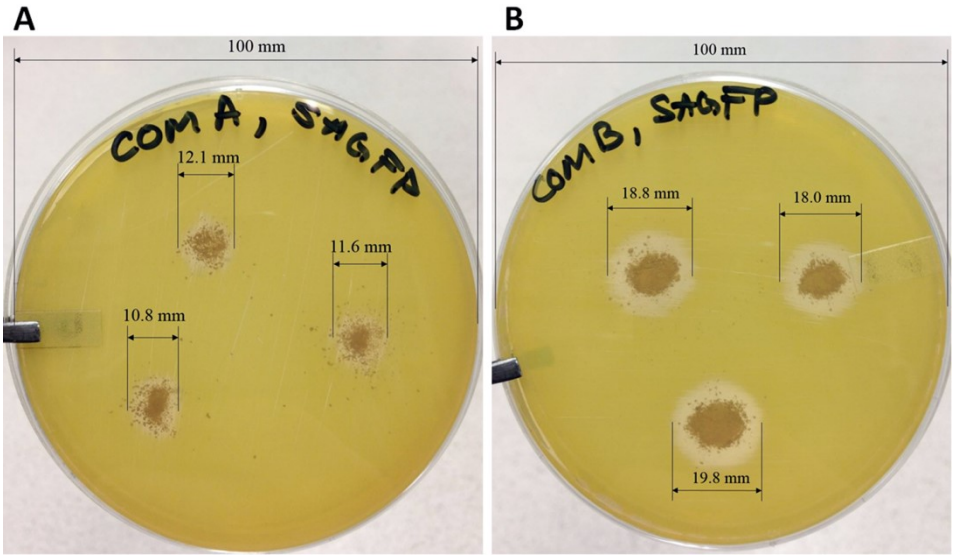

Figure 3. CompA (A) and CompB (B) inhibit the planktonic growth of *S. aureus* strain AH133. The analysis was done using the ZOI assay.

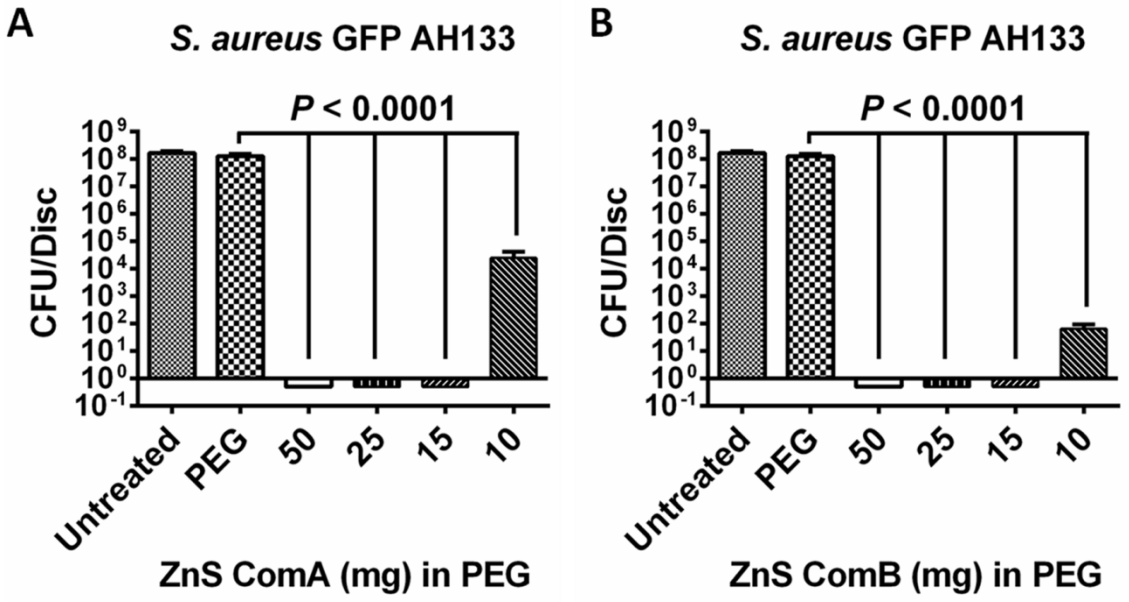

Figure 4. ZnS ointment inhibits biofilm development by the *S. aureus* strain AH133. Cellulose disks were inoculated with AH133 and covered with pieces of sterile gauze containing either CompA-formulated ointment (A) or CompB-formulated ointment (B). Some disks were covered with pieces of sterile gauze containing PEG (ointment

control) while others were covered with sterile gauze (untreated controls). Values represent the means (plus/minus) SE of three independent experiments.

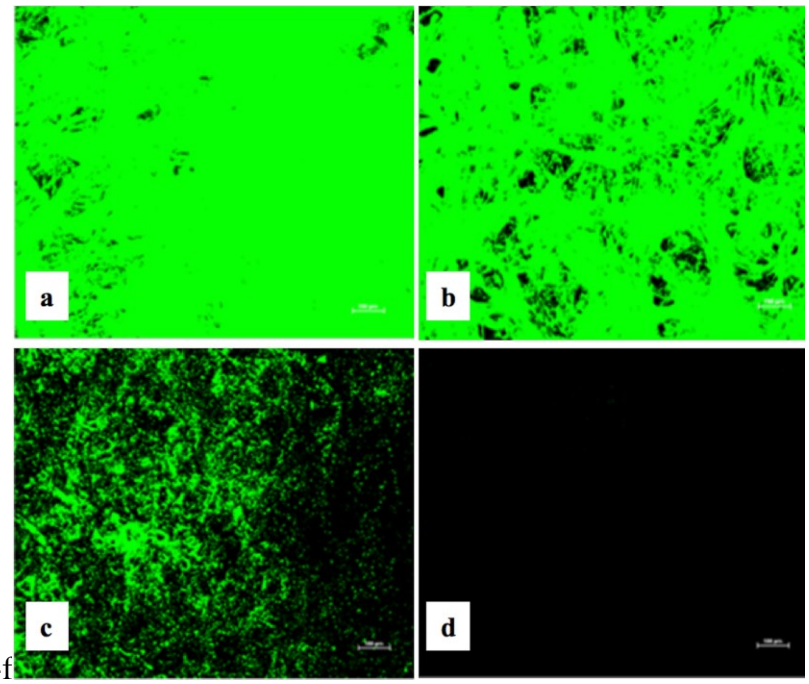

-f

Figure 5. CLSM visualization of the biofilm formed on disks inoculated with AH133 and treated with either CompA-formulated ointment (A) or CompB ormulated ointment (B). a, untreated control; b, discs treated with PEG (cream base); c, discs treated with 10 mg of CompA (A); d, discs treated with 10 mg of CompB (B). Experiments were conducted as described in Figure 4.

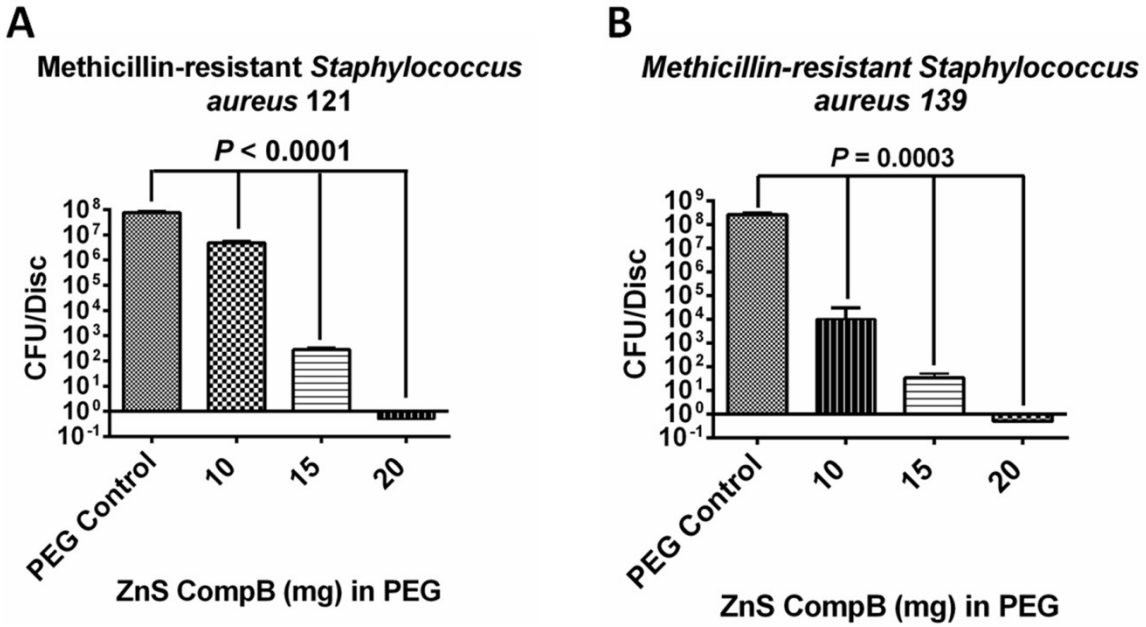

Figure 6. CompB-formulated cream inhibits biofilm development by the *S. aureus* methicillin resistant (MRSA) clinical isolates 121 (A) and 139 (B). Experiments were

conducted as described in Figure 4. Disks were treated with 10, 15, or 20 mg of CompB-formulated in PEG. Values represent the means of three independent experiments (plus/minus) SE.